

Sustainable synthesis of carbon nanomaterials from waste tire-derived char using microwave pyrolysis

Amani Hussein Sharaf Addin^{1,2*}, Raihan Mahirah Ramli^{1,2*}, Suriati Sufian^{1,2},
Najib Al-Mahbashi³ , Siti Shawalliah Idris⁴, Abid Salam Farooqi^{1,2},
Shakimi Haikal Shamsu Bakri^{1,2}

¹ Centre of Innovative Nanostructures & Nanodevices (COINN), Institute of Smart and Sustainable Living, Universiti Teknologi PETRONAS, 32610 Seri Iskandar, Perak, Malaysia

² Chemical Engineering Department, Universiti Teknologi PETRONAS, 32610 Seri Iskandar, Perak, Malaysia

³ Civil and Environmental Engineering Department, Universiti Teknologi PETRONAS, 32610 Perak, Malaysia

⁴ School of Chemical Engineering, College of Engineering, Universiti Teknologi MARA, 40450 Shah Alam, Selangor

* Corresponding author's e-mail: amani_22011516@utp.edu.my; raihan.ramli@utp.edu.my

ABSTRACT

The increasing accumulation of non-biodegradable waste tires poses significant environmental challenges, necessitating innovative recycling solutions. This study investigates the use of waste tire-derived char (WTRC) for the synthesis of carbon nanomaterials (CNMs) through microwave-assisted pyrolysis. Waste tire rubber crumbs (WTRCs) were pyrolyzed at 600 W for 20 minutes to produce char, which was subsequently purified and utilized as a precursor for CNMs synthesis. CNMs were synthesized using tire-derived char and ferrocene as a catalyst at varying microwave power levels (600–1000 W), reaction times (10–40 min), and catalyst-to-precursor ratios (25–100 wt%). Comprehensive characterization techniques, including FT-IR, XRD, Raman spectroscopy, TEM, and FESEM, revealed that Carbon nanofibers (CNFs) synthesized at 1000 W under optimal conditions exhibited bamboo-shaped, tubular structures with diameters ranging from 425 to 881 nm. XRD confirmed the graphitic nature of the CNFs, while Raman spectroscopy indicated a moderate degree of graphitization ($ID/IG = 1.61$). TEM analysis confirmed a tip-growth mechanism, where residual iron-based catalyst nanoparticles were embedded at the tips of the fibers, promoting CNFs elongation. FESEM analyses showed residual iron-based catalyst particles embedded within the CNFs, highlighting the importance of further refining synthesis conditions to enhance purity. These CNFs, with their porous structure and high surface area, hold potential for adsorption-based applications such as wastewater treatment and pollutant removal.

Keywords: carbon nanomaterials, carbon nanofibers, microwave-assisted pyrolysis, sustainable waste tire recycling, tire-derived char.

INTRODUCTION

The rapid increase in global waste tire production, driven by rising automobile usage, presents a growing environmental challenge as an estimated 17 million tons of waste tires are discarded annually, with projections suggesting this could reach 1.2 billion tons per year by the 2030s (Jahirul et al., 2021). The non-biodegradable nature of rubber, coupled with its

resistance to physical, chemical, and biological degradation, allows waste tires to persist in the environment for decades, making their disposal a significant concern (Alkhatib, 2015; Jahirul et al., 2021). However, waste tires are highly rich in carbon content (approximately 88%) and are composed of a mixture of elastomers, including natural rubber, styrene, butadiene, and styrene-butadiene rubbers. They also contain metal reinforcements, such as zinc and sulfur, along with carbon fillers/strengtheners and other compatible additives (Jones et al., 2021). Tire pyrolysis can recover up to 90% of carbon

residue, which can be used for advanced material synthesis (Mwafy, 2020).

On the other hand, Carbon Nanomaterials (CNMs), such as carbon nanotubes (CNTs) and carbon nanofibers (CNFs), are widely utilized in various industrial applications, such as biosensors, gas sensors, batteries, and capacitors (Anis et al., 2018; Dixit et al., 2017; Tahir et al., 2018). Their unique combination of properties (i.e., exceptional tensile strength, outstanding thermal and electrical conductivity, and a high length-to-diameter ratio) makes them highly versatile materials (Choo et al., 2012; Parmar et al., 2023).

Sufficient research exists on utilizing waste tires as a carbon source through catalytic pyrolysis and chemical vapor deposition (CVD) methods for synthesizing CNMs (Li et al., 2019; Mwafy, 2020). One of the significant limitations of traditional pyrolysis is heating, which is neither cost-effective nor economically viable. Sustainable production of CNMs (Parmar et al., 2023). On the other hand, microwave (MW) heating is fast and cost-effective due to its unique heating mechanism. It penetrates directly into materials, heating them efficiently without significantly affecting the surroundings, leading to substantial energy savings (Mishra and Sharma, 2016). As a result, MW-assisted pyrolysis is an innovative, fast, and energy-efficient approach. While significant research has focused on synthesizing CNMs using microwave pyrolysis from plastic and biomass waste (Parmar et al., 2023; Baghel and Kaushal, 2022; Yuwen et al., 2023a) (Hildago-Oporto et al., 2019; Yuwen et al., 2023b), limited studies have explored its application to waste tires as a carbon source.

In this study, we investigated the synthesis of CNMs from waste tire-derived char using microwave-assisted pyrolysis. Waste tire rubber crumbs were processed to produce high-carbon char, which served as the precursor for CNMs synthesis. By optimizing key parameters, such as microwave power, radiation time, and catalyst ratio, this study successfully demonstrated the potential of microwave-assisted pyrolysis for producing CNMs from waste tire-derived char. Comprehensive characterization techniques, including XRD, Raman spectroscopy, TEM, and FESEM, were employed to evaluate the structural and morphological properties of the synthesized CNMs produced under optimized conditions.

MATERIALS AND METHODS

Materials

Waste tires Rubber crumbs (WTRCs) were thoroughly washed with clean water to eliminate dust and impurities, followed by drying in an electric oven at 80°C for 24 hours. The dried material was then sieved to obtain particles within the size range of 0.4–0.6 mm. Ferrocene ($Fe(C_5H_5)_2$) was employed as a catalyst precursor. Acetone (CH_3COCH_3), a volatile and efficient organic solvent, was used to remove residual organic impurities from the char. Hydrochloric acid (HCl, 37% w/v) was employed to eliminate inorganic ash residues through acid washing. All chemicals were of analytical grade and sourced from Sigma-Aldrich, Malaysia.

Experimental procedure

Char production

The Char was produced using a modified multimode microwave system (1.5 kW, 2.45 GHz) equipped with a quartz glass reactor featuring nitrogen gas inlet and outlet ports. WTRCs served as the precursor material, with 20 g of WTRCs loaded into the quartz reactor. The reactor was purged with nitrogen gas at a flow rate of 100 mL/min for 10 minutes to establish an inert atmosphere.

Pyrolysis was performed at an optimized microwave power of 600 W and a residence time of 20 minutes, based on prior research demonstrating these conditions yield a high fixed carbon content (Bing et al., 2021). The resulting char was washed sequentially with acetone to dissolve organic impurities, leveraging its high efficiency and ease of evaporation, followed by dilute hydrochloric acid to eliminate inorganic ash residues. The purified char was then dried in an oven at 105 °C and stored for subsequent carbon nanomaterial (CNM) synthesis. The yield of char was calculated using Equation 1:

$$\begin{aligned} \text{Solid char yield (\%)} &= \\ &= \frac{\text{Mass of solid char}}{\text{Mass of raw crumb sample}} \times 100\% \end{aligned} \quad (1)$$

CNMs synthesis

Carbon nanomaterials (CNMs) were synthesized using the same microwave system employed for char production. Waste tire-derived char served as the carbon precursor, while ferrocene acted as

the catalyst. These components were blended in varying weight ratios (25 wt% to 100 wt%) and loaded into a quartz glass reactor placed within the microwave system (Karaeva et al., 2020).

Microwave synthesis experiments were performed at power levels ranging from 600 W to 1000 W and radiation times spanning 10 to 40 minutes to investigate the influence of process parameters on CNMs formation. To establish an inert atmosphere, the reactor was purged with nitrogen gas at a flow rate of 100 mL/min for 10 minutes prior to microwave irradiation. Nitrogen flow was maintained throughout the reaction to prevent oxidation and ensure consistent synthesis conditions (Mubarak et al., 2014).

Characterization techniques

WTRCs and resulting Char

A comprehensive proximate analysis of WTRCs was conducted to determine moisture content, volatile matter, fixed carbon, and ash content, following standard ASTM procedures. Moisture content was measured by drying the samples at 105 °C to a constant weight, while volatile matter was determined by heating the samples in a closed crucible at 950 °C. Fixed carbon was calculated as the remaining fraction after accounting for moisture, volatile matter, and ash, with ash content quantified by combusting the samples at 750 °C for 3 hours (Wang et al., 2019). Elemental analysis of WTRCs was performed using an elemental analyzer (Elementar VarioMicro) to determine the content of carbon (C), hydrogen (H), nitrogen (N), and sulfur (S). Oxygen (O) was calculated by difference. All measurements were conducted in duplicate to ensure accuracy and reproducibility (Urrego-Yepes et al., 2021).

The surface morphology of the char and the chemical element composition was examined using scanning electron microscopy (SEM) (Zeiss EVO LS15) equipped with energy-dispersive X-ray spectroscopy (EDS). SEM micrographs provided detailed insights into the structural and textural properties of the char (Mistar et al., 2020). Functional groups and chemical bonds in the char were identified using Fourier-transform infrared spectroscopy (FTIR) (PerkinElmer Spectrum One, USA). Samples were prepared as KBr pellets and analysed over the wavenumber range of 4000–400 cm^{-1} . The FTIR spectra provided insight into the chemical composition, highlighting functional groups essential for understanding the reactivity and potential applications of the char (Xu et al., 2018).

Synthesized CNMs

The synthesized CNMs were thoroughly characterized to evaluate their morphology, structure, and crystallinity. Field-emission scanning electron microscopy (FESEM) (Zeiss Supra V55) was employed to examine the surface morphology and confirm nanomaterials formation (Raza et al., 2020). Before imaging, the samples were coated with a thin gold layer via sputtering to enhance conductivity and improve resolution. XRD (Panalytical X'Pert3 Powder) was used to analyse the crystalline structure of the carbon nanofibers (CNFs), providing insights into their phase composition and degree of crystallinity. Raman spectroscopy (Horiba Jobin Yvon HR) was performed to assess the graphitization degree and defect density within the CNFs, a critical parameter in the evaluation (Kure et al., 2022). Detailed structural features, including wall arrangement and tube alignment, were visualised using transmission electron microscopy (TEM) (Hitachi HT7830), which provided high-resolution imaging of CNT morphology (Tan et al., 2016).

RESULTS AND DISCUSSION

Proximate and ultimate analysis of WTRCs

The proximate analysis (Table 1) reveals a low moisture content (0.14%), indicating minimal water presence, while the material consists predominantly of volatile matter (59.82%) and fixed carbon (27.77%), with a notable ash content of 12.28%. These values reflect the thermal stability and combustion properties of the rubber crumbs (Reyes Rodriguez et al., 2019).

The ultimate analysis shows a high carbon content (79.16%), suggesting significant energy potential, complemented by a substantial hydrogen content (7.427%). Nitrogen (2.26%) and sulphur (0.062%) are present in minor amounts, while oxygen and other elements (calculated by difference) constitute 11.091%. These elemental compositions are crucial for evaluating the suitability of rubber crumbs in applications such as pyrolysis, energy recovery, or material recycling (Chen et al., 2019).

Characterizations of solid char

The chemical composition of the char was analysed using FTIR, as shown in Figure 1. The FTIR spectra reveal significant changes in

Table 1. Proximate and elemental composition analysis of rubber crumbs

Proximate analysis (%)		Ultimate analysis (%)	
Moisture	0.14	Carbon	79.16
Ash	12.28	Hydrogen	7.427
Volatile matter	59.82	Nitrogen	2.26
Fixed carbon	27.77	Sulphur	0.062
		Oxygen + others (By difference)	11.091

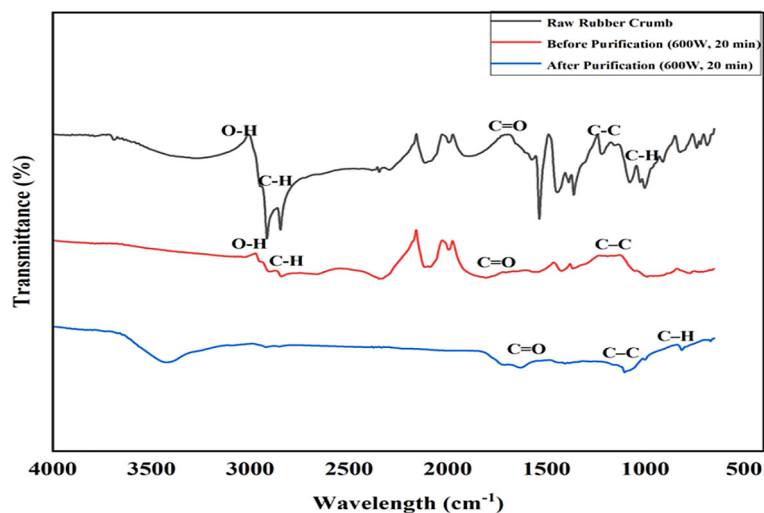


Figure 1. FTIR spectra of raw rubber crumb, char before purification, and char after purification (600 W, 20 min)

functional groups during pyrolysis and purification. The broad -OH peak (~3400 cm⁻¹) decreased significantly after purification with acetone and HCl, confirming the effective removal of oxygen-containing functional groups and impurities, resulting in a carbon-rich char (Nunes and Pardini, 2019). The raw rubber crumb exhibited strong aliphatic -CH peaks (~2900 cm⁻¹), which diminished after pyrolysis, indicating the removal of organic components (Moreno-Castilla et al., 2000). Additionally, the band in the region from 1650 cm⁻¹ to 1860 cm⁻¹, associated with C=O stretching vibrations corresponding to carbonyl and carboxyl groups, became more

pronounced after purification, indicating surface activation of the char (Gómez-Hernández et al., 2019; Moreno-Castilla et al., 2000). Peaks in the region from 800 cm⁻¹ to 1200 cm⁻¹ correspond to C–C stretching vibrations (Wibawa et al., 2020). Bands below 950 cm⁻¹ are attributed to out-of-plane deformation vibrations of C–H groups in aromatic structures, supporting the presence of aromatic frameworks in the purified char (Moreno-Castilla et al., 2000).

The surface morphology of the char was examined using SEM, as shown in Figure 2. At 400 W, the char exhibited a smooth surface with minimal porosity, indicating incomplete carbonization (Yu et

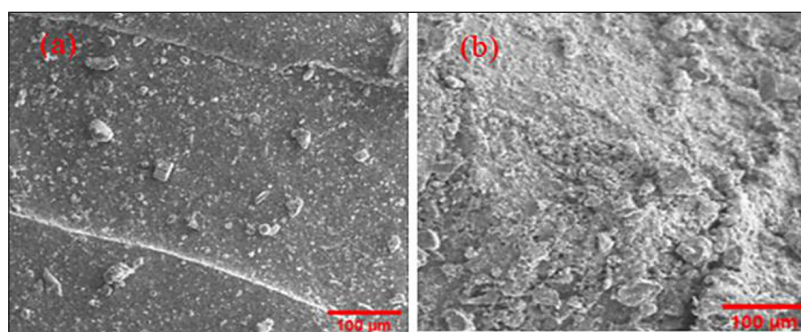


Figure 2. SEM images of char produced at 400 W (a) and 600 W (b) at 200 × magnification

al., 2010). In contrast, the 600 W char displayed a rougher, more porous structure, reflecting enhanced carbonization (Maiti et al., 2006; Wahi et al., 2016). Similar studies that used char as a precursor for CNMs synthesis found that increased porosity is essential for effective metal catalyst dispersion and carbon diffusion, leading to improved CNMs formation (Baghel and Kaushal, 2022; Hidalgo et al., 2023; Hildago-Oporto et al., 2019). Although higher microwave powers (e.g., 800 W and 1000 W) were tested, they resulted in significantly reduced char yields. This reduction can be attributed to secondary reactions, where the increased thermal energy promotes further decomposition of primary volatile products into gaseous compounds (Khan et al., 2022). As a result, 600 W was identified as the optimal condition, balancing yield and structural quality to produce a suitable precursor for CNMs synthesis.

As shown in Figure 3, EDX analysis revealed an increase in carbon content from 79.27 wt% at 400 W to 83.37 wt% at 600 W, indicating improved carbonization (Jiang et al., 2023). The reduction in oxygen content reflects the removal of volatile components, while small amounts of sulfur, zinc, and silicon likely originate from the rubber crumb feedstock (Selvarajoo and Oochit, 2020; Song et al., 2017). These results confirm that higher microwave power enhances elemental purity and yields carbon-rich char.

Effect of synthesis conditions

The effect of synthesis parameters, including microwave power, radiation time, and catalyst loading, on the yield and chemical structure

of the products was evaluated. Microwave power significantly influences CNMs synthesis. At 600 W and 800 W, the reactor temperatures (250 °C and 520 °C) were insufficient for CNFs growth, resulting primarily in the formation of amorphous carbon. Low microwave power was reported to result in small catalyst sizes and reduced carbon atom diffusion rates, hindering nanostructure formation. Conversely, higher microwave power increased the size of the Fe catalyst and enhanced carbon diffusion, supporting the formation of filamentous carbon (Irfan et al., 2023). Additionally, low power may partially deactivate the catalyst, further preventing filamentous carbon synthesis (Yao et al., 2019). However, an increase in microwave power also led to a decrease in CNMs yield, which may be attributed to excessive fragmentation or volatilization of carbon precursors at high temperatures (Abdelsayed et al., 2019)

Radiation time significantly influences CNMs synthesis, with CNFs formation observed only at the maximum radiation time of 40 min in this study. Shorter radiation times (10–30 minutes) primarily yielded amorphous carbon, likely due to insufficient time for complete carbon atom diffusion and catalyst activation (Schwenke et al., 2015). It has been demonstrated that extending the microwave radiation time enhances the growth of filamentous carbon, as prolonged exposure provides the conditions necessary for the effective development of carbon nanofibers (CNFs) (Omoriyekomwan et al., 2022). Furthermore, the quality of the char, serving as the hydrocarbon source, is a critical factor in determining the efficiency of filamentous carbon formation. This

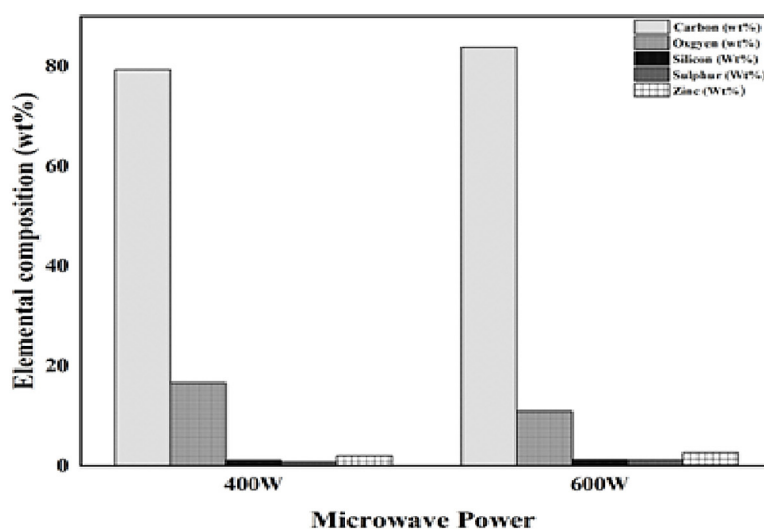


Figure 3. Elemental composition (wt%) of char produced at 400 W and 600 W

highlights the importance of optimizing both radiation time and the precursor material for successful filamentous carbon synthesis (Baghel and Kaushal, 2022; Hildago-Oporto et al., 2019; Wulan and Setiawati, 2018).

Catalyst loading played a significant role in CNMs synthesis by influencing the availability of active sites for carbon deposition. A 1:1 feedstock-to-catalyst ratio facilitated the synthesis of CNFs; however, the CNFs produced under this condition exhibited impurities, likely due to residual catalyst particles. This aligns with previous findings, where iron-based catalysts, demonstrated effective carbon formation for CNT synthesis at the same loading ratio (Yuwen et al., 2023a; Zhao et al., 2024). In addition to catalyst loading, catalyst type also significantly influenced CNFs morphology, as shown in Table 2. Fe-based catalysts favored bamboo-like CNFs, while biomass-derived catalysts resulted in tubular or hollow CNFs.

Characterization of CNMs

FTIR analysis of CNMs

The FTIR spectra of the samples at different microwave power levels (Figure 4) reveal significant changes in functional groups. The samples are referred to as amorphous carbon at 600 W (CNMs-600), amorphous carbon at 800 W (CNMs-800), and carbon nanofibers at 1000 W (CNFs-1000), respectively. The broad peak at 3400 cm^{-1} , associated with O–H stretching vibrations, decreases significantly at 1000 W. This reduction indicates the removal of oxygen-containing functional groups (Voiry et al., 2016). Peaks in the $3000\text{--}2800\text{ cm}^{-1}$

range, corresponding to C–H stretching vibrations of aliphatic hydrocarbons, decrease in intensity with increasing microwave power, indicating the scission of hydrocarbon chains (Miller et al., 2021). Additionally, bands at 1561 cm^{-1} and 1150 cm^{-1} , attributed to the graphitic structure of carbon nanofibers (CNFs), are observed in all spectra but become significantly more pronounced in the 1000 W sample (Liu et al., 2005). This increased intensity at 1000 W correlates with the successful formation of CNFs, as confirmed by FESEM analysis. Peaks below 1000 cm^{-1} , linked to C–H deformation and aromatic vibrations, confirm the presence of aromatic frameworks in the carbon structures (Moreno-Castilla et al., 2000).

Morphological analysis (FESEM)

The surface morphology of the carbon structures synthesized under varying conditions was examined using FESEM, as shown in Figures 5 and 6. At 800 W for 25 minutes with 62.5 wt% catalyst loading (Figure 5), the resulting structures predominantly consisted of amorphous carbon with spherical or granular morphology. The formation of amorphous carbon under these conditions can be attributed to insufficient microwave power and suboptimal reaction temperatures, which limit the activation of the catalyst and the diffusion of carbon atoms onto its surface (Hildago-Oporto et al., 2019). As noted by Wang *et al.* (2020) higher temperatures and controlled pressure conditions are essential for facilitating CNT growth, while deviations from these parameters often lead to the formation of more amorphous carbon.

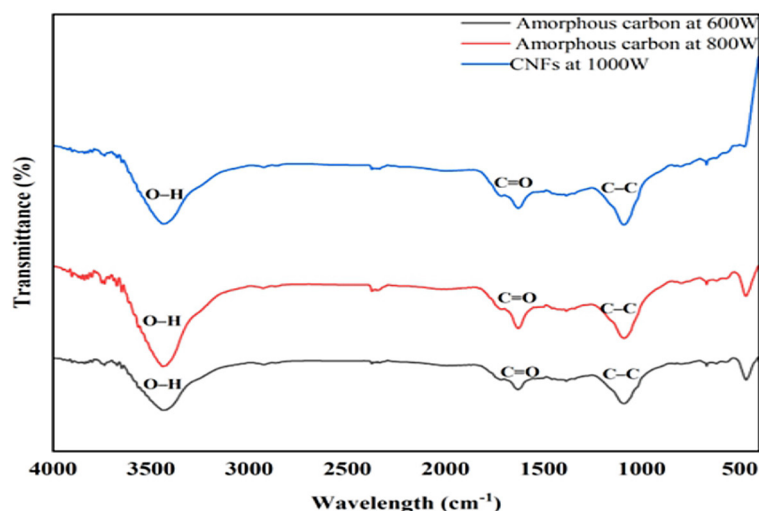


Figure 4. FTIR spectra of amorphous carbon at 600 W and 800 W, and CNFs at 1000 W

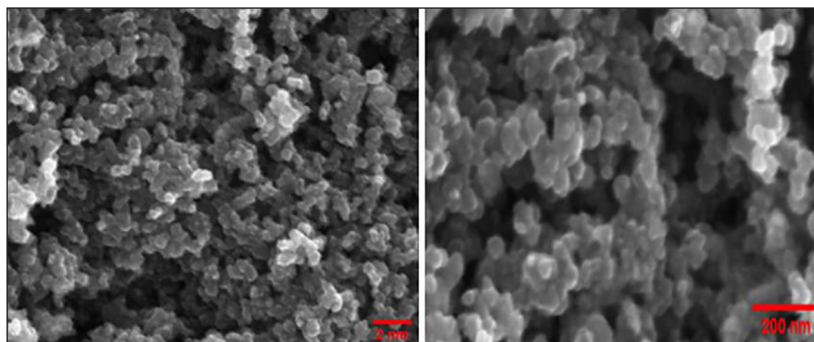


Figure 5. FESEM images of carbon structures synthesized at 800 W for 25 minutes with 62.5 wt% catalyst: (a) 30k magnification, (b) 50k magnification

In contrast, carbon nanofibers (CNFs) were successfully synthesized at 1000 W for 40 minutes with 100 wt% catalyst loading (Figure 6). The FESEM images reveal threadlike, curved, and entangled tubular structures with diameters in the range of approximately 425–881 nm, indicating uniformity in CNFs formation. These findings align with previous studies on microwave pyrolysis of various carbon-rich plastic feedstocks, such as polypropylene (PP), high-density polyethylene (HDPE), and low-density polyethylene (LDPE), which also employed high microwave power to synthesize CNFs and CNTs (Irfan et al., 2023; Shen et al., 2022; Yuwen et al., 2023b). The higher microwave power and extended radiation time provided sufficient energy to activate the catalyst and sustain carbon diffusion, enabling the growth of well-structured CNFs (Omoriyekomwan et al., 2019). Additionally, Small amounts of catalyst impurities, likely iron-based, were observed on the surface, as corroborated by XRD analysis and further supported by TEM imaging and Raman spectroscopy.

Structural characterization (XRD)

The X-ray diffraction (XRD) pattern of CNFs synthesized at 1000 W for 40 minutes is shown in

Figure 7. The XRD analysis reveals two prominent diffraction peaks at approximately 26° and 43° , which correspond to the (002) and (100) planes of graphitic carbon, indicating the existence of a crystalline graphite structure within these CNFs (Baghel and Kaushal, 2022). The strong and broad peaks of CNFs, as reported by Kamil et al. (2014), were observed at the (002) plane, showing a slight downward shift to an angle of 26.5° , which corresponds to the C=C inter-layer spacing characteristic of sp^2 hybridization. Meanwhile, the peak around 43° corresponds to the (100) plane, further corroborating the presence of crystalline carbon materials.

A notable peak near 44° is attributed to iron carbide (Fe-C), confirming the presence of residual catalyst particles in the sample (Hidalgo et al., 2023). The presence of Fe-C phases has also been reported in other microwave pyrolysis studies using Fe-based catalysts, where metal residues play a role in CNFs or CNTs and structural defects (Shen et al., 2022; Yuwen et al., 2023b). Additionally, low-intensity peaks in the XRD pattern suggest the presence of amorphous carbon, which is often associated with incomplete graphitization during the synthesis process (Theodorakopoulos

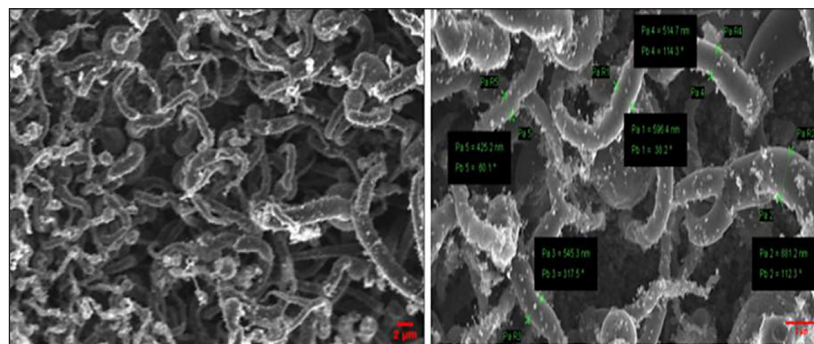


Figure 6. FESEM images of CNFs synthesized at 1000 W for 40 minutes with 100 wt% catalyst: (a) 10.0 k magnification, (b) 5.0 k magnification

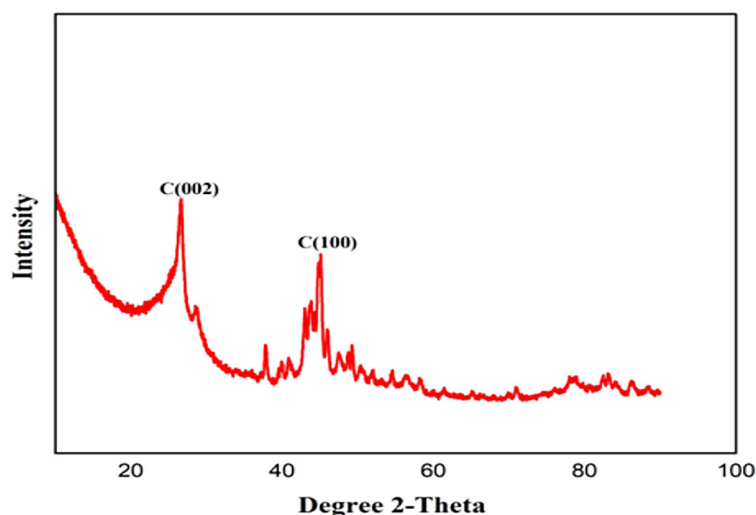


Figure 7. X-ray diffraction pattern of CNFs synthesized at 1000 W for 40 minutes

et al., 2024). These results align with the formation of filamentous carbon structures (CNFs) rather than cylindrical carbon nanotubes, as also supported by the FESEM analysis.

Raman spectroscopy

Raman spectroscopy is commonly used to identify the quality or graphitic nature of carbons based on the intensity of D and G bands (Jorio and Souza Filho, 2016; Theofanidis et al., 2016; Zhang and Williams, 2016). The D-band in the Raman shift indicates amorphous or disordered carbon, arising from structural defects and associated with sp^3 -hybridized carbon (Yang et al., 2019). In contrast, the G-band represents graphitic or filamentous carbon, indicative of ordered

structures and associated with sp^2 -hybridized carbon (He et al., 2021). From Figure 8, the Raman spectrum shows the D-band at 1350 cm^{-1} and the G-band at 1587 cm^{-1} .

The ratio between the size of the D and G peaks provides a quantitative measure of the degree of graphitisation in carbon materials (Yao et al., 2022). The low I_D/I_G ratio (≤ 1.0) indicates better graphitisation, signifying higher purity of carbon nanomaterials (CNMs) with fewer defects (Zhang et al., 2023). Conversely, a high I_D/I_G ratio suggests a greater defect density and lower graphitization (Chaudhary et al., 2018). From Figure 8, the Raman spectrum shows an I_D/I_G ratio of 1.61, which is relatively high, indicating a moderate degree of graphitisation. This result can be attributed to

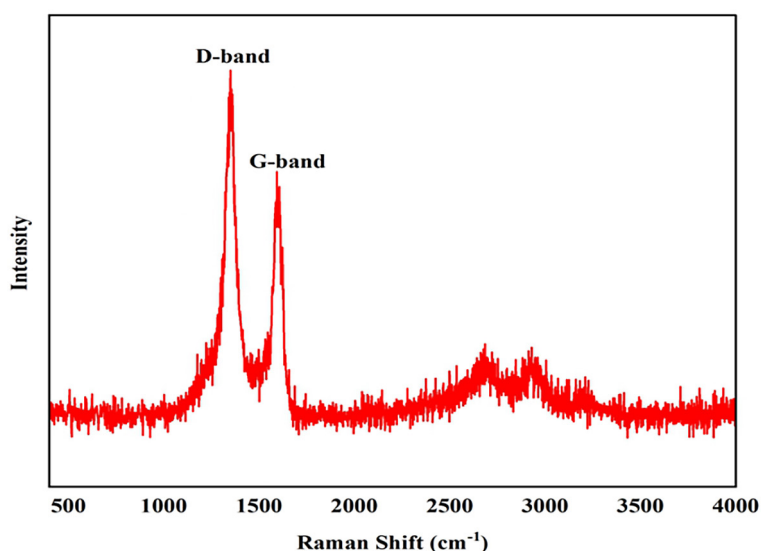


Figure 8. Raman spectrum of CNFs synthesized at 1000 W for 40 minutes

the high catalyst-to-precursor ratio used during the synthesis, which likely increased the fraction of Fe in the iron-based catalysts. A higher Fe content is known to limit the precipitation efficiency of carbon during microwave pyrolysis, leading to the formation of CNFs with poor crystallinity (Yuwen et al., 2023b). The presence of iron-based catalyst impurities, as revealed in the FESEM analysis, aligns with the Raman results, further supporting the observed moderate crystallinity in the CNFs

TEM analysis

The TEM images (Figure 9) provide a detailed view of the internal structure of the CNFs synthesized at 1000 W for 40 minutes with a 1:1 catalyst-to-precursor ratio, as captured at varying magnification levels. The micrographs confirm that the synthesized carbon structures are bamboo-shaped CNFs, characterized by their tubular morphology, which is consistent with similar findings reported in earlier literature (Monthieux et al., 2007; Parmar et al., 2023).

In Figure 9(B), the dark spots correspond to residual catalyst particles embedded within

the carbon nanostructures. These nanoparticles are distributed along the CNFs, particularly at the tips and in the middle of the nanofibers, which suggests a tip-growth mechanism during the synthesis process (Parmar et al., 2023; Yao et al., 2022). Similar studies that used iron-based catalysts for CNTs or CNFs synthesis also observed a tip-growth mechanism, where catalyst nanoparticles facilitate carbon diffusion at the fiber tips, promoting longitudinal growth (Yuwen et al., 2023a; Zhang et al., 2022; Zhao et al., 2024). This growth process may be attributed to the effects of microwave irradiation during synthesis. Microwave irradiation electrically charges the iron nanoparticles, generating localized electric currents and high voltages at the tips, which facilitates carbon atom alignment and diffusion to the catalyst surface (Zhan et al., 2017).

The dark spots, indicative of metal impurities, also suggest the significant presence of iron-based catalyst residues within the CNFs. This observation is corroborated by the FESEM, XRD, and Raman analyses, which confirm the presence of iron-based impurities on the surface of the CNFs.

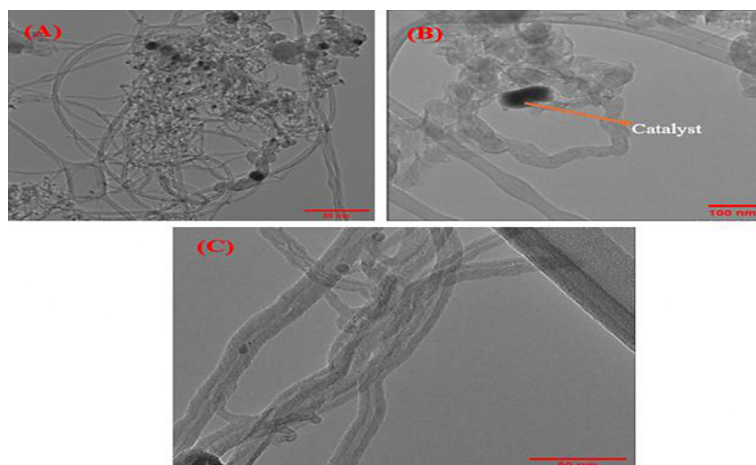


Figure 9. TEM images of CNFs synthesized at 1000 W for 40 minutes: (a) 30k, (b) 80k, and (c) 200k magnification

Table 2. Comparison of CNMs synthesized via microwave pyrolysis from different carbon precursors

Carbon source	Microwave conditions	Catalyst	CNFs morphology	I _D /I _G Ratio	Reference
Waste Tires	1000 W, 40 min	Ferrocene	Bamboo-like, entangled CNFs	1.61	This study
Polyethylene	900 W, 30 min	10% Ni/Al ₂ O ₃	bamboo-shaped CNFs	1.08	Parmar et al., 2023
Palm kernel shell	600 °C, and 20 min	Mineral in the biomass	Tubular and bamboo-shaped CNFs	0.95	Omoriyekomwan et al., 2017
Pine nutshell	400–700 °C, 20 min	Mineral in the biomass	Hollow carbon nanofibers	0.8	J. Zhang et al., 2018
Polyolefin plastic	600–1200 W, 5 min	MAX (Ti ₃ AlC ₂)	filamentous carbon nanofibers	0.88	Cao et al., 2022

CONCLUSIONS

Waste tire-derived char was successfully utilized as a precursor material for the synthesis of carbon nanomaterials through microwave-assisted pyrolysis. Char produced at 600 W for 20 minutes underwent purification to remove impurities and oxygen-containing functional groups, resulting in a carbon-rich precursor with enhanced structural integrity and reactivity. Using this precursor and ferrocene as a catalyst, CNMs were synthesized under varying conditions of microwave power (600–1000 W), reaction times (10–40 minutes), and catalyst-to-precursor ratios (25–100 wt%).

The optimized synthesis conditions of 1000 W microwave power, 40 minutes irradiation, and 100 wt% catalyst loading produced uniform bamboo-shaped CNFs with diameters ranging from 425 to 881 nm. Characterization techniques, including FTIR, XRD, Raman spectroscopy, TEM, and FESEM, confirmed the formation of graphitic CNFs with crystalline structures and a moderate degree of graphitisation ($I_D/I_G = 1.61$). TEM images revealed residual iron-based catalyst particles embedded within the nanofibers, suggesting a tip-growth mechanism during synthesis. Lower microwave power levels (600 W and 800 W) resulted in amorphous carbon due to insufficient energy for catalyst activation and carbon diffusion.

Despite the moderate crystallinity, the synthesized CNFs exhibit a high surface area and porous structure, making them suitable for adsorption-based applications, such as wastewater treatment, pollutant removal, and gas adsorption. This study demonstrates the potential of microwave-assisted pyrolysis as a sustainable and efficient approach for converting waste tire-derived char into advanced carbon nanomaterials.

Acknowledgement

The authors gratefully acknowledge the financial support provided by Universiti Teknologi PETRONAS, Malaysia, through the Yayasan Universiti Teknologi PETRONAS (YUTP) under grant number 015LC0-534, as well as the University Internal Research Funding (URIF) under grant number 015LB0-123.

REFERENCES

1. Abdelsayed, V., Ellison, C. R., Trubetskaya, A., Smith, M. W., & Shekhawat, D. (2019). Effect of microwave and thermal co-pyrolysis of low-rank coal and pine wood on product distributions and char structure. *Energy and Fuels*, 33(8). <https://doi.org/10.1021/acs.energyfuels.9b01105>
2. Alkhatib, R. (2015). Development of an alternative fuel from waste of used tires by pyrolysis. *MINES Nantes, l'U Nam*.
3. Anis, B., Mostafa, A. M., El Sayed, Z. A., Khalil, A. S. G., & Abouelsayed, A. (2018). Preparation of highly conductive, transparent, and flexible graphene/silver nanowires substrates using non-thermal laser photoreduction. *Optics and Laser Technology*, 103. <https://doi.org/10.1016/j.optlastec.2018.01.057>
4. Baghel, P., & Kaushal, P. (2022). Rapid synthesis of carbon nanotubes from Prosopis Juliflora bio-char using microwave irradiation. *Materials Science and Engineering: B*, 286. <https://doi.org/10.1016/j.mseb.2022.115987>
5. Bing, W., Hongbin, Z., Zeng, D., Yuefeng, F., Yu, Q., & Rui, X. (2021). Microwave fast pyrolysis of waste tires: Effect of microwave power on product composition and quality. *Journal of Analytical and Applied Pyrolysis*, 155. <https://doi.org/10.1016/j.jaap.2020.104979>
6. Cao, Q., Dai, H. C., He, J. H., Wang, C. L., Zhou, C., Cheng, X. F., & Lu, J. M. (2022). Microwave-initiated MAX Ti3AlC2-catalyzed upcycling of polyolefin plastic wastes: Selective conversion to hydrogen and carbon nanofibers for sodium-ion battery. *Applied Catalysis B: Environmental*, 318. <https://doi.org/10.1016/j.apcatb.2022.121828>
7. Chaudhary, S. K., Singh, K. K., & Venugopal, R. (2018). Study about characterization of CNTs through electron microscopy and Raman spectroscopy. *IOP Conference Series: Materials Science and Engineering*, 377(1). <https://doi.org/10.1088/1757-899X/377/1/012122>
8. Chen, R., Li, Q., Zhang, Y., Xu, X., & Zhang, D. (2019). Pyrolysis kinetics and mechanism of typical industrial non-tyre rubber wastes by peak-differentiating analysis and multi kinetics methods. *Fuel*, 235. <https://doi.org/10.1016/j.fuel.2018.08.121>
9. Choo, H., Jung, Y., Jeong, Y., Kim, H. C., & Ku, B.-C. (2012). Fabrication and applications of carbon nanotube fibers. *Carbon Letters*, 13(4). <https://doi.org/10.5714/cl.2012.13.4.191>
10. Dixit, S., Singhal, S., Vankar, V. D., & Shukla, A. K. (2017). Size dependent Raman and absorption studies of single walled carbon nanotubes synthesized by pulse laser deposition at room temperature. *Optical Materials*, 72. <https://doi.org/10.1016/j.optmat.2017.07.008>

11. Gómez-Hernández, R., Panecatl-Bernal, Y., & Méndez-Rojas, M. Á. (2019). High yield and simple one-step production of carbon black nanoparticles from waste tires. *Heliyon*, 5(7). <https://doi.org/10.1016/j.heliyon.2019.e02139>
12. He, S., Xu, Y., Zhang, Y., Bell, S., & Wu, C. (2021). Waste plastics recycling for producing high-value carbon nanotubes: Investigation of the influence of Manganese content in Fe-based catalysts. *Journal of Hazardous Materials*, 402. <https://doi.org/10.1016/j.jhazmat.2020.123726>
13. Hidalgo, P., Navia, R., Hunter, R., Camus, C., Buschmann, A., & Echeverria, A. (2023). Carbon nanotube production from algal biochar using microwave irradiation technology. *Journal of Analytical and Applied Pyrolysis*, 172. <https://doi.org/10.1016/j.jaap.2023.106017>
14. Hildago-Oporto, P., Navia, R., Hunter, R., Coronado, G., & Gonzalez, M. E. (2019). Synthesis of carbon nanotubes using biochar as precursor material under microwave irradiation. *Journal of Environmental Management*, 244, 83–91. <https://doi.org/10.1016/j.jenvman.2019.03.082>
15. Hon Tan, W., Lee, S. L., Ng, J. H., Fong Chong, W. W., & Chong, C. T. (2016). Characterization of carbon nanotubes synthesized from hydrocarbon-rich flame. *International Journal of Technology*, 7(2). <https://doi.org/10.14716/ijtech.v7i2.3284>
16. Irfan, M., Saleem, R., Shoukat, B., Hussain, H., Shukrullah, S., Naz, M. Y., Rahman, S., Ghanim, A. A. J., Nawalany, G., & Jakubowski, T. (2023). Production of combustible fuels and carbon nanotubes from plastic wastes using an in-situ catalytic microwave pyrolysis process. *Scientific Reports*, 13(1). <https://doi.org/10.1038/s41598-023-36254-6>
17. Jahirul, M. I., Hossain, F. M., Rasul, M. G., & Chowdhury, A. A. (2021). A review on the thermochemical recycling of waste tyres to oil for automobile engine application. In *Energies* 14(13). <https://doi.org/10.3390/en14133837>
18. Jiang, H., Shao, J., Zhu, Y., Yu, J., Cheng, W., Yang, H., Zhang, X., & Chen, H. (2023). Production mechanism of high-quality carbon black from high-temperature pyrolysis of waste tire. *Journal of Hazardous Materials*, 443. <https://doi.org/10.1016/j.jhazmat.2022.130350>
19. Jones, I., Zhu, M., Zhang, J., Zhang, Z., Preciado-Hernandez, J., Gao, J., & Zhang, D. (2021). The application of spent tyre activated carbons as low-cost environmental pollution adsorbents: A technical review. In *Journal of Cleaner Production* 312. Elsevier Ltd. <https://doi.org/10.1016/j.jclepro.2021.127566>
20. Jorio, A., & Souza Filho, A. G. (2016). Raman Studies of Carbon Nanostructures. In *Annual Review of Materials Research* (Vol. 46). <https://doi.org/10.1146/annurev-matsci-070115-032140>
21. Kamil, A. M., Hussein, F. H., Halbus, A. F., & Bahnamann, D. W. (2014). Preparation, characterization, and photocatalytic applications of MWCNTs/TiO₂ composite. *International Journal of Photoenergy*, 2014. <https://doi.org/10.1155/2014/475713>
22. Karaeva, A., Urvanov, S., Kazennov, N., Mitberg, E., & Mordkovich, V. (2020). Synthesis, Structure and Electrical Resistivity of Carbon Nanotubes Synthesized over Group VIII Metallocenes. *Nanomaterials*, 10(11). <https://doi.org/10.3390/nano10112279>
23. Khan, M. A., Hameed, B. H., Siddiqui, M. R., Alothman, Z. A., & Alsohaimi, I. H. (2022). Comparative investigation of the physicochemical properties of chars produced by hydrothermal carbonization, pyrolysis, and microwave-induced pyrolysis of food waste. *Polymers*, 14(4). <https://doi.org/10.3390/polym14040821>
24. Kure, N., Daniel, I. H., Hamidon, N. M., Lakin, I. I., Machu, B. U., & Adoyi, E. J. (2022). Effect of time on the syntheses of carbon nanotubes via domestic oven. *Journal of the Nigerian Society of Physical Sciences*, 4(1). <https://doi.org/10.46481/jnsps.2022.355>
25. Li, W., Wei, M., Liu, Y., Ye, Y., Li, S., Yuan, W., Wang, M., & Wang, D. (2019). Catalysts evaluation for production of hydrogen gas and carbon nanotubes from the pyrolysis-catalysis of waste tyres. *International Journal of Hydrogen Energy*, 44(36), 19563–19572. <https://doi.org/10.1016/j.ijhydene.2019.05.204>
26. Liu, M., Yang, Y., Zhu, T., & Liu, Z. (2005). Chemical modification of single-walled carbon nanotubes with peroxytrifluoroacetic acid. *Carbon*, 43(7). <https://doi.org/10.1016/j.carbon.2005.01.023>
27. Maiti, S., Dey, S., Purakayastha, S., & Ghosh, B. (2006). Physical and thermochemical characterization of rice husk char as a potential biomass energy source. *Bioresource Technology*, 97(16). <https://doi.org/10.1016/j.biortech.2005.10.005>
28. Miller, D. D., Smith, M. W., & Shekhawat, D. (2021). Microwave-induced selective decomposition of cellulose: Computational and experimental mechanistic study. *Journal of Physics and Chemistry of Solids*, 150. <https://doi.org/10.1016/j.jpcs.2020.109858>
29. Mishra, R. R., & Sharma, A. K. (2016). Microwave-material interaction phenomena: Heating mechanisms, challenges and opportunities in material processing. In *Composites Part A: Applied Science and Manufacturing* 81. <https://doi.org/10.1016/j.compositesa.2015.10.035>
30. Mistar, E. M., Alfatah, T., & Supardan, M. D. (2020). Synthesis and characterization of activated carbon from *Bambusa vulgaris striata* using two-step KOH activation. *Journal of Materials Research and Technology*, 9(3). <https://doi.org/10.1016/j.jmrt.2020.03.001>

- jmrt.2020.03.041
31. Monthieux, M., Noé, L., Dussault, L., Dupin, J. C., Latorre, N., Ubieto, T., Romeo, E., Royo, C., Monzón, A., & Guimon, C. (2007). Texturising and structuring mechanisms of carbon nanofilaments during growth. *Journal of Materials Chemistry*, 17(43). <https://doi.org/10.1039/b707742d>
 32. Moreno-Castilla, C., López-Ramón, M. V., & Carrasco-Marín, F. (2000). Changes in surface chemistry of activated carbons by wet oxidation. *Carbon*, 38(14). [https://doi.org/10.1016/S0008-6223\(00\)00048-8](https://doi.org/10.1016/S0008-6223(00)00048-8)
 33. Mubarak, N. M., Sahu, J. N., Abdullah, E. C., Jayakumar, N. S., & Ganesan, P. (2014). Single stage production of carbon nanotubes using microwave technology. *Diamond and Related Materials*, 48. <https://doi.org/10.1016/j.diamond.2014.07.005>
 34. Mwafy, E. A. (2020). Eco-friendly approach for the synthesis of MWCNTs from waste tires via chemical vapor deposition. *Environmental Nanotechnology, Monitoring and Management*, 14. <https://doi.org/10.1016/j.enmm.2020.100342>
 35. Nunes, K. S. D., & Pardini, L. C. (2019). Purification and characterization methods for lignin biomass as a potential precursor for carbon materials. *Cellulose Chemistry and Technology*, 53(3–4). <https://doi.org/10.35812/cellulosechemtechnol.2019.53.23>
 36. Omoriyekomwan, J. E., Tahmasebi, A., Zhang, J., & Yu, J. (2017). Formation of hollow carbon nanofibers on bio-char during microwave pyrolysis of palm kernel shell. *Energy Conversion and Management*, 148, 583–592. <https://doi.org/10.1016/j.enconman.2017.06.022>
 37. Omoriyekomwan, J. E., Tahmasebi, A., Zhang, J., & Yu, J. (2019). Mechanistic study on direct synthesis of carbon nanotubes from cellulose by means of microwave pyrolysis. *Energy Conversion and Management*, 192, 88–99. <https://doi.org/10.1016/j.enconman.2019.04.042>
 38. Omoriyekomwan, J. E., Tahmasebi, A., Zhang, J., & Yu, J. (2022). Synthesis of super-long carbon nanotubes from cellulosic biomass under microwave radiation. *Nanomaterials*, 12(5). <https://doi.org/10.3390/nano12050737>
 39. Parmar, K. R., Pant, K. K., & Roy, S. (2021). Blue hydrogen and carbon nanotube production via direct catalytic decomposition of methane in fluidized bed reactor: Capture and extraction of carbon in the form of CNTs. *Energy Conversion and Management*, 232. <https://doi.org/10.1016/j.enconman.2021.113893>
 40. Parmar, K. R., Tuli, V., Caiola, A., Hu, J., & Wang, Y. (2023). Sustainable production of hydrogen and carbon nanotubes/nanofibers from plastic waste through microwave degradation. *International Journal of Hydrogen Energy*. <https://doi.org/10.1016/j.ijhydene.2023.08.224>
 41. Raza, M. M. H., Sadiq, M., Khan, S., Zulfequar, M., Husain, M., Husain, S., & Ali, J. (2020). A single step in-situ process for improvement in electron emission properties of surface-modified carbon nanotubes (CNTs): Titanium dioxide nanoparticles attachment. *Diamond and Related Materials*, 110. <https://doi.org/10.1016/j.diamond.2020.108139>
 42. Reyes Rodriguez, D. A., Reyes Trejos, O. Y., & Camargo Vargas, G. de J. (2019). Evaluation of the pyrolysis and co-pyrolysis process of palm shell and waste tyres in a CO₂ atmosphere. *Avances Investigación En Ingeniería*, 16(2). <https://doi.org/10.18041/1794-4953/avances.2.5501>
 43. Sayyed, A. J., Pinjari, D. V., Sonawane, S. H., Bhanvase, B. A., Sheikh, J., & Sillanpää, M. (2021). Cellulose-based nanomaterials for water and wastewater treatments: A review. In *Journal of Environmental Chemical Engineering* 9(6). <https://doi.org/10.1016/j.jece.2021.106626>
 44. Schwenke, A. M., Hoepfener, S., & Schubert, U. S. (2015). Microwave synthesis of carbon nanofibers—the influence of MW irradiation power, time, and the amount of catalyst. *Journal of Materials Chemistry A*, 3(47). <https://doi.org/10.1039/c5ta06937h>
 45. Selvarajoo, A., & Oochit, D. (2020). Effect of pyrolysis temperature on product yields of palm fibre and its biochar characteristics. *Materials Science for Energy Technologies*, 3. <https://doi.org/10.1016/j.mset.2020.06.003>
 46. Shen, X., Zhao, Z., Li, H., Gao, X., & Fan, X. (2022). Microwave-assisted pyrolysis of plastics with iron-based catalysts for hydrogen and carbon nanotubes production. *Materials Today Chemistry*, 26. <https://doi.org/10.1016/j.mtchem.2022.101166>
 47. Song, Z., Yang, Y., Sun, J., Zhao, X., Wang, W., Mao, Y., & Ma, C. (2017). Effect of power level on the microwave pyrolysis of tire powder. *Energy*, 127. <https://doi.org/10.1016/j.energy.2017.03.150>
 48. Tahir, M. B., Nabi, G., Iqbal, T., Sagir, M., & Rafique, M. (2018). Role of MoSe₂ on nanostructures WO₃-CNT performance for photocatalytic hydrogen evolution. *Ceramics International*, 44(6). <https://doi.org/10.1016/j.ceramint.2018.01.081>
 49. Theodorakopoulos, G. V., Karousos, D. S., Benra, J., Forero, S., Hammerstein, R., Sapalidis, A. A., Katsaros, F. K., Schubert, T., & Favvas, E. P. (2024). Well-established carbon nanomaterials: modification, characterization and dispersion in different solvents. *Journal of Materials Science*, 59(8). <https://doi.org/10.1007/s10853-024-09413-x>
 50. Theofanidis, S. A., Batchu, R., Galvita, V. V., Poelman, H., & Marin, G. B. (2016). Carbon gasification from Fe-Ni catalysts after methane dry reforming. *Applied Catalysis B: Environmental*, 185. <https://doi.org/10.1016/j.apcatb.2015.12.006>
 51. Urrego-Yepes, W., Cardona-Urbe, N., Vargas-Isaza,

- C. A., & Martínez, J. D. (2021). Incorporating the recovered carbon black produced in an industrial-scale waste tire pyrolysis plant into a natural rubber formulation. *Journal of Environmental Management*, 287. <https://doi.org/10.1016/j.jenvman.2021.112292>
52. Voiry, D., Yang, J., Kupferberg, J., Fullon, R., Lee, C., Jeong, H. Y., Shin, H. S., & Chhowalla, M. (2016). High-quality graphene via microwave reduction of solution-exfoliated graphene oxide. *Science*, 353(6306). <https://doi.org/10.1126/science.aah3398>
53. Wahi, R., Abdul Aziz, S. M., Hamdan, S., & Ngaini, Z. (2016). Biochar production from agricultural wastes via low-temperature microwave carbonization. *RFM 2015 - 2015 IEEE International RF and Microwave Conference*. <https://doi.org/10.1109/RFM.2015.7587754>
54. Wang, J., Shen, B., Lan, M., Kang, D., & Wu, C. (2020). Carbon nanotubes (CNTs) production from catalytic pyrolysis of waste plastics: The influence of catalyst and reaction pressure. In *Catalysis Today* 351, 50–57. Elsevier B.V. <https://doi.org/10.1016/j.cattod.2019.01.058>
55. Wang, M., Zhang, L., Li, A., Irfan, M., Du, Y., & Di, W. (2019). Comparative pyrolysis behaviors of tire tread and side wall from waste tire and characterization of the resulting chars. *Journal of Environmental Management*, 232, 364–371. <https://doi.org/10.1016/j.jenvman.2018.10.091>
56. Wibawa, P. J., Nur, M., Asy'ari, M., & Nur, H. (2020). SEM, XRD and FTIR analyses of both ultrasonic and heat generated activated carbon black microstructures. *Heliyon*, 6(3). <https://doi.org/10.1016/j.heliyon.2020.e03546>
57. Wulan, P. P. D. K., & Setiawati, N. S. (2018). The Effect of Mass Ratio of Ferrocene to Camphor as Carbon Source and Reaction Time on the Growth of Carbon Nanotubes. *E3S Web of Conferences*, 67. <https://doi.org/10.1051/e3sconf/20186703037>
58. Xu, F., Wang, B., Yang, D., Ming, X., Jiang, Y., Hao, J., Qiao, Y., & Tian, Y. (2018). TG-FTIR and Py-GC/MS study on pyrolysis mechanism and products distribution of waste bicycle tire. *Energy Conversion and Management*, 175. <https://doi.org/10.1016/j.enconman.2018.09.013>
59. Yang, W., Jiang, Z., Hu, X., Li, X., Wang, H., & Xiao, R. (2019). Enhanced activation of persulfate by nitric acid/annealing modified multi-walled carbon nanotubes via non-radical process. *Chemosphere*, 220. <https://doi.org/10.1016/j.chemosphere.2018.12.136>
60. Yao, C., Bai, W., Geng, L., He, Y., Wang, F., & Lin, Y. (2019). Experimental study on microreactor-based CNTs catalysts: Preparation and application. *Colloids and Surfaces A: Physicochemical and Engineering Aspects*, 583. <https://doi.org/10.1016/j.colsurfa.2019.124001>
61. Yao, L., Yi, B., Zhao, X., Wang, W., Mao, Y., Sun, J., & Song, Z. (2022). Microwave-assisted decomposition of waste plastic over Fe/FeAl₂O₄ to produce hydrogen and carbon nanotubes. *Journal of Analytical and Applied Pyrolysis*, 165. <https://doi.org/10.1016/j.jaap.2022.105577>
62. Yu, F., Steele, P. H., & Ruan, R. (2010). Microwave pyrolysis of corn cob and characteristics of the pyrolytic chars. *Energy Sources, Part A: Recovery, Utilization and Environmental Effects*, 32(5). <https://doi.org/10.1080/15567030802612440>
63. Yuwen, C., Liu, B., Rong, Q., Hou, K., Zhang, L., & Guo, S. (2023a). Enhanced microwave absorption capacity of iron-based catalysts by introducing Co and Ni for microwave pyrolysis of waste COVID-19 Masks. *Fuel*, 340. <https://doi.org/10.1016/j.fuel.2023.127551>
64. Yuwen, C., Liu, B., Rong, Q., Hou, K., Zhang, L., & Guo, S. (2023b). Mechanism of microwave-assisted iron-based catalyst pyrolysis of discarded COVID-19 masks. *Waste Management*, 155, 77–86. <https://doi.org/10.1016/j.wasman.2022.10.041>
65. Zhan, M., Pan, G., Wang, Y., Kuang, T., & Zhou, F. (2017). Ultrafast carbon nanotube growth by microwave irradiation. *Diamond and Related Materials*, 77. <https://doi.org/10.1016/j.diamond.2017.06.001>
66. Zhang, J., Tahmasebi, A., Omoriyekomwan, J. E., & Yu, J. (2018). Direct synthesis of hollow carbon nanofibers on bio-char during microwave pyrolysis of pine nut shell. *Journal of Analytical and Applied Pyrolysis*, 130, 142–148. <https://doi.org/10.1016/j.jaap.2018.01.016>
67. Zhang, P., Liang, C., Wu, M., Chen, X., Liu, D., & Ma, J. (2022). High-efficient microwave plasma discharging initiated conversion of waste plastics into hydrogen and carbon nanotubes. *Energy Conversion and Management*, 268. <https://doi.org/10.1016/j.enconman.2022.116017>
68. Zhang, P., Wu, M., Liang, C., Luo, D., Li, B., & Ma, J. (2023). In-situ exsolution of Fe-Ni alloy catalysts for H₂ and carbon nanotube production from microwave plasma-initiated decomposition of plastic wastes. *Journal of Hazardous Materials*, 445. <https://doi.org/10.1016/j.jhazmat.2022.130609>
69. Zhang, Y., & Williams, P. T. (2016). Carbon nanotubes and hydrogen production from the pyrolysis catalysis or catalytic-steam reforming of waste tyres. *Journal of Analytical and Applied Pyrolysis*, 122. <https://doi.org/10.1016/j.jaap.2016.10.015>
70. Zhao, J., Gao, J., Wang, D., Chen, Y., Zhang, L., Ma, W., & Zhao, S. (2024). Microwave-intensified catalytic upcycling of plastic waste into hydrogen and carbon nanotubes over self-dispersing bimetallic catalysts. *Chemical Engineering Journal*, 483. <https://doi.org/10.1016/j.cej.2024.149270>